Colloids and Surfaces A: Physicochem. Eng. Aspects 423 (2013) 178–187

Contents lists available at SciVerse ScienceDirect

Colloids and Surfaces A: Physicochemical and Engineering Aspects

journal homepage: www.elsevier.com/locate/colsurfa

Experimental determination of the colloidal stability of Fe(III)-montmorillonite: Effects of organic matter, ionic strength and pH conditions

Laura Borgnino*

Centro de Investigaciones en Ciencias de la Tierra (CICTERRA). Instituto de Investigaciones en Físico-Química Córdoba (INFIQC). Departamento de Fisicoquímica, Facultad de Ciencias Químicas. Universidad Nacional de Córdoba. Ciudad Universitaria, 5000, Córdoba, Argentina

HIGHLIGHTS

- Low pH and high ionic strength may destabilize Fe-M suspensions.
- High concentrations of AH stabilize suspensions of Fe-M.
- For all pH, steric and electrostatic effects have an influence on Fe-M stabilization.
- The steric effects are more important at pH 4.5 and high ionic strength.
- The DLVO energy profiles support the experimental results.

GRAPHICAL ABSTRACT

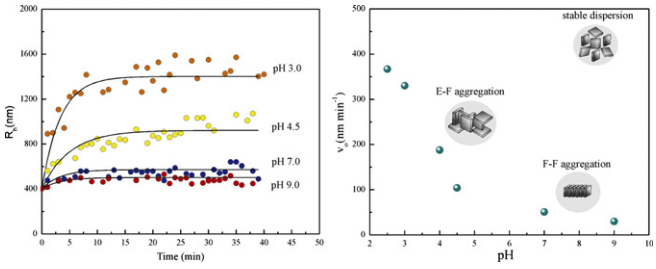

ARTICLE INFO

Article history:
Received 21 December 2012
Received in revised form 28 January 2013
Accepted 30 January 2013
Available online xxx

Keywords:
Aggregation
Humic acid
Fe(III)-montmorillonite
Colloidal stability

ABSTRACT

Aggregation and disaggregation of particle colloids are one of the most important surface-driven phenomena encountered in the aquatic and terrestrial environments and a key factor controlling a number of important environmental processes. This study investigates the effects of pH, ionic strength, and humic acid concentration on the stability behavior of Fe(III)-montmorillonite, a natural colloid commonly present in natural waters. Time-resolved dynamic light scattering was used to monitor the increase of the aggregate size over time in the aggregation kinetics experiments. Aggregation rate, stability ratio, and CCC (critical coagulation concentration) were calculated to quantify the experimental results, and the DLVO theory was employed to explain the observed behaviors. The effect of humic acid on the colloidal electrosteric stability was also investigated. This study demonstrates that low pH and high ionic strength may destabilize Fe(III)-montmorillonite suspensions, while increasing humic acid concentrations has the opposite effect, stabilizing the suspension at any pH. Comparing the steric and electrostatic effects on the Fe-M stabilization, both have an important influence for all pH levels studied, although steric is more pronounced at low pH and high ionic strength. DLVO energy predictions support the experimental results. The obtained results contribute to the understanding of the behavior of colloidal particles in saline or freshwater natural environments as well as the role of humic acid in the mobility of contaminants associated with natural colloids.

1. Introduction

The occurrence of natural colloids (particles with an effective diameter of less than 10 μm) is very common in natural aquatic media [1]. Both natural waters such as lakes and streams and pore water found in sediments and soils contain natural colloids and dissolved ions. A variety of organic and inorganic materials exist as colloids, including humic substances, "biocolloids" such as microorganisms, mineral precipitates, and weathering products. The occurrence of colloids may be detrital (contained in the original parent geologic material) or authigenic (formed *in situ* through geochemical alteration of primary mineral solids) [2]. Layer silicates,

* Corresponding author. Tel.: +54 351 4334169/4; fax: +54 351 4334188.
E-mail address: borgnino@fcq.unc.edu.ar

0927-7757/$ – see front matter © 2013 Elsevier B.V. All rights reserved.
http://dx.doi.org/10.1016/j.colsurfa.2013.01.065

as well as iron and aluminum oxides, can be detrital in subsurface sediments, while secondary hydrous oxides, silica, calcite and other complex mixtures and solid solutions of theses phases are authigenic colloidal particles [2]. Regardless of their origin, dispersed colloids can remain a stable suspension in water. Due to their small size, they do not settle by gravitation. Furthermore, at the pH values of natural water, the particles are charged; so the electrostatic interactions, the van der Waals forces, and the steric forces maintain the stability of the colloidal suspension. Any changes in such a system with respect to pH, ion concentrations, or other factors may destabilize the suspension. Besides, colloids have a large specific surface area which makes them an important absorbent in natural waters. Hence, their potential to affect and modify the transport of many pollutants in natural aquatic systems is significant [1,2,3].

The colloidal mobility depends on its stability. To be mobile over a distance and thus facilitate contaminant transport, suspended colloidal material must be resistant to aggregation with other similar particles. Aggregation, the process of producing large aggregates by collisions induced by interparticle motion, is an important process which occurs among colloids. Although nanoparticles have been recently the focus of the aggregation studies [4–8] the importance of the aggregation process has been documented during decades [2,9–16]. Colloid stabilization is influenced by the particle mineralogy, surface charges, and by the extent of the electrical double layer. According to the theory proposed by Derjaguin and Landau, [17] Verwey and Overbeek [18], (DLVO theory), the stability of a homogeneous colloidal suspension is determined by the balance between van der Waals attractive forces that promote aggregation, and by electrostatic repulsive forces that drive particles apart. Studies have shown that aggregation causes rapid deposition of suspended sediments in rivers and may change the sediment transport properties, both in terms of the particle size and floc density [19,20]. Another consequence of aggregation is that fewer surface sites could be available for adsorption. Thus, aggregation and disaggregation also impacts the sorption–desorption of contaminants, and therefore in the transport in the aquatic media.

A number of studies have been conducted to evaluate the aggregation behavior of natural colloids particles via dynamic light scattering. Many of them involve experimental studies on the effect of ionic strength, pH and organic matter in the aggregation of oxide nanoparticles [5–8,21–25]. Fewer studies focused in the aggregation of clay minerals particles [26–30] and less in a theoretical and experimental approach of the effects of humic acid on the aggregation of clays [16,31,32] or Fe(III) modified clays.

The goals of this study are to investigate the stability of a Fe(III)-montmorillonite at different pH and ionic strength conditions, and the effect of humic acid on its stabilization using dynamic light scattering. A series of batch experiments were conducted to measure the hydrodynamic size of Fe(III)-montmorillonite via dynamic light scattering under a variety of experimental conditions. Aggregation rate, stability ratio, and critical coagulation concentration were estimated using the experimental results, and the DLVO theory was employed to explain the observed behaviors. Because sediment particle's composition is mostly clay minerals, Fe/Mn (hydr) oxide and organic matter which often exists as coating of clays, the system Fe(III)-montmorillonite employed in this work is used with the intention of representing the colloid behaviour of natural sediments particles. The obtained results may contribute to describe the behavior of colloids particles in saline or freshwater natural environments, as well as to understand the role that humic acid plays in the mobility of contaminants associated with natural colloids.

2. Material and methods

All solutions were prepared from analytical reagent grade chemicals and purified water (Milli-Q system).

2.1. Fe(III)-montmorillonite (Fe-M) and humic acid (HA) samples

The Fe-M sample employed was the same one used in previous research [33,34,35]. 550 mL of a clear fresh solution were mixed with 250 mL of a 2.2% Na-M dispersion in water, whose pH was adjusted to 3.5 before the mixing. After 2 h of vigorous magnetic stirring at this pH, a NaOH solution was added drop wise until pH 9. Once at pH 9, the dispersion was stirred for other 3 h and then the solid was washed with water and dried at 60 °C for 3 days. The chemical and mineralogical characteristics of the Fe-M obtained were described elsewhere [33]. The solid had an iron content of 77.3 mg g^{-1} and a specific surface area of 567 m^2 g^{-1}, measured by the methylene blue adsorption method [36]. More than 60% of the total Fe(III) in this sample corresponded to interlayer/sorbed Fe(III) as XRD pattern and Mössbauer spectra indicated. The remaining fraction was already present in Na-M (structural Fe). If some ferrihydrite was formed as an associated phase, it has not been detected in the diffraction pattern [33].

HA suspensions were prepared from a Fluka humic acid (code: 1415-93-6), which had been previously purified according to the methodology proposed by the International Humic Substances Society [37]. Once the purification was completed, a concentrated stock solution of 2 g L^{-1} was prepared by dissolving a weighted amount of HA at pH 10 during 2 h. The HA stock solution was stored in dark conditions at 5 °C.

2.2. Aggregation kinetic measurements

The aggregation kinetics of the Fe-M and Fe-M-HA suspensions was investigated by the time-resolved dynamic light scattering (DLS) measurements (Delsa Nano 2.20, Beckman Coulter Inc.). The equipment was operated at a controlled temperature (25 ± 1 °C) and all light scattering experiments were conducted at 165° scattering angle. Using DLS, the average hydrodynamic radius R_h of the aggregates was measured as a function of time t. From the diffusion coefficient, the R_h could then be calculated using the Stokes–Einstein equation: $R_h = k_B T/6\pi\eta D$ where k_B is the Boltzmann constant, T is the absolute temperature, and η is the viscosity of the medium. The method of cumulants was used to extract the average diffusion coefficient from the intensity autocorrelation functions [31].

For the aggregation kinetics experiments, the increase of the R_h with time was recorded. The initial change in particle radius with time (the aggregation rate constant) is proportional to the particle concentration [38]. It is difficult to determine the absolute aggregation rate constants for the suspensions of nonspherical, polydispersed particles, such as montmorillonite. However, aggregation rates are often expressed in relative terms as the so-called stability ratio, W, by normalizing them to the rate of fast aggregation. Therefore, for a series of suspensions having the same mass concentration and the same initial particle sizes, W can be determined directly from the initial slopes of aggregation curves as:

$$W = \frac{[(dR_h/dt)_{t\to 0}/C]^{(f)}}{[(dR_h/dt)_{t\to 0}/C]} \quad (1)$$

where $(dR_h/dt)_{t\to 0}$ is the initial change in particle radius with time (in nm min^{-1}), C is the particle mass concentration (in mg L^{-1}), and (f) indicates the regime of fast aggregation, as explained below.

For each experiment, a dilute suspension containing 8.0–20.0 mg L^{-1} of Fe-M was prepared in a 0.01 M $NaNO_3$ electrolyte solution at the desired pH. The suspensions were agitated to maximize particle dispersion. A subsample was then quickly transferred into a glass cuvette; where R_h was monitored for 40 min and a complete autocorrelation function was recorded every 60 s. Aggregation rate constants were calculated from

the initial slope of the ratio between the hydrodynamic mean radius and time, $(dR_h/dt)_{t\to 0}$. Because of the lag time between sample preparation (pH adjusted and agitation) and the first measurement of R_h was approximately 1–2 min; a correction scheme was implemented to include the initial aggregation values in the analysis. Firstly, a simple kinetic equation was used to fit experimental data. This process was performed only for the purpose of simulating the kinetic aggregation curve, especially in the initial stage of aggregation which is very rapid and where less data were available. After that, the slope of the function was extrapolated to the time where R_h is equal to the initial particle size. This process is usually conducted over a time range from $t = 0$ until the time at which $R_h(t)$ reaches $1.25\,R_{h0}$ [22,27,39], where R_{h0} (=402 nm) is the initial hydrodynamic radius from the stable Fe-M suspension, determined by DLS method. For all the cases evaluated, the value of the hydrodynamic radius extrapolated through the linear regression to $t = 0$ is within 20 nm of R_{h0} [22,27]. In cases where extremely rapid aggregation takes place, especially at higher electrolyte concentrations (0.04 and 0.05 M) and low pH (pH < 4.5), the regression analysis was performed to values greater than $1.25\,R_{h0}$ ($\backsim 2.5\,R_{h0}$), and therefore more data are available to calculate the initial rates.

The effects of suspension pH and ionic strength on the aggregation kinetics of Fe-M were studied by conducting experiments at different pH (4.5, 7.0, and 9.0) in $NaNO_3$ solutions of varying ionic strengths (0.01, 0.02 and 0.04 M). Suspensions containing 20 mg L^{-1} of Fe-M were prepared and adjusted to the desired pH values by appropriate additions of HNO_3 or NaOH. The aggregation was followed as described and the pH of the suspension was not corrected during the experiment.

In addition, a set of experiments was conducted to establish the initial slope of the aggregation curves in the regime of fast aggregation. In this case, a suspension of Fe-M (20 mg L^{-1}) in 0.05 M $NaNO_3$ solution at pH 4 was prepared, and aggregation was monitored as described above. The initial aggregation rate from these experiments, obtained as was previously mentioned, was used to calculate the stability for all other samples according to Eq. (1).

To investigate the influence of HA on the aggregation of Fe-M, a suspension containing 20 mg L^{-1} of Fe-M with 2, 10, and 20 mg L^{-1} of HA was prepared. The pH suspension was adjusted to 4.5, 7.0, and 9.0 by additions of HNO_3 or NaOH, and the ionic strength was varied over the same range, as varied in the Fe-M aggregation experiments.

2.3. Zeta potential (ζ)

The zeta potential measurements were carried out using the Delsa Nano Size (Beckman) apparatus. Fe-M suspensions (20 mg L^{-1}) were prepared by dispersing the samples in 0.01, 0.02, and 0.04 M of $NaNO_3$. The suspension pH was raised to approximately 9 with NaOH, and the zeta potential measurement was carried out. After that, the pH was slightly decreased with HNO_3 and a new measurement was performed. This procedure was continued until the pH reached approximately 3.5. To investigate the effect of HA on the zeta potential of Fe-M particle suspension, the same procedure was repeated by preparing a suspension containing 20 mg L^{-1} of Fe-M with 2 and 20 mg L^{-1} of HA.

2.4. DLVO theory: particle–particle interaction energy

The DLVO theory [17,18] was applied in this study to provide a theoretical framework to explain the aggregation behavior of the Fe-M suspension under different ionic strengths and pH condition, in the presence or absence of different HA concentrations. The total potential energy of interaction is the sum of two contributions, the electrostatic double layer repulsion (V_{el}) and van der Waals attraction (V_{VDW}):

$$V_t = V_{el} + V_{VDW} \tag{2}$$

In the case of identical spherical particles ($r_1 = r_2$ and $\zeta_1 = \zeta_2$), low potential and large values of double layer thickness, the electrical double layer repulsive energy [40] and the van der Waals attractive energy [41] are expressed as the following:

$$V_{el} = 2\pi\varepsilon\varepsilon_0 r\zeta^2 \ln(1 + e^{-\kappa He}) \tag{3}$$

$$V_{VDW} = -\frac{A}{12}\left[\frac{1}{x^2+2x} + \frac{1}{x^2+2x+1} + 2\ln\frac{x^2+2x}{x^2+2x+1}\right] \tag{4}$$

The Eq. (4) is the complete Hamaker expression where $x = H/2r$, A (J) is the Hamaker constant, H is the particle interdistance, r (m) is the radius of particles, $\varepsilon\varepsilon_0$ is the dielectric permittivity of the solution, and κ (m^{-1}) is the reciprocal double layer thickness. The zeta potential of the charged particles, ζ, is assumed to equal the surface potential [42] and, as an estimate value of particle radius, the experimental value of R_h was used. The effective separation (H_E) for the interacting particles is given by [41]:

$$H_e = H - 2s\,[\mathrm{m}] \tag{5}$$

where H is the particle interdistance and s is the Stern layer thickness. A value of 0.1 nm was chosen, which could be estimated from the half interdistance between plates of Fe(III)-montmorillonite in water with a (d_{001}) basal spacing of 11.45 Å [33], after subtracting the alumino-silicate plate thickness of 0.95 nm [43].

The Hamaker constant (A) is an intrinsic property of the material that the colloidal particles are composed, in the solvent that are dispersed. It is indicative of the strength of long-range mutual attraction between two small volumes of the material. In this study, the value of $7.30\,E^{-21}$ J was used, which had been previously proposed for the face-to-edge montmorillonite surface interaction [44]. Because clay aggregation is predominantly face-to edge, this value is adequacy to be used in the calculation of the van der Waals attractive energy.

The contribution of HA to the stabilization of Fe-M particles was also investigated and modeled with a simple model of steric stabilization. HA is expected to adsorb onto edge surface of Fe(III)-montmorillonite, alters the physicochemical properties and thus the interfacial forces/energies between them. It has been suggested that HA might introduce a steric force [45] and a bridging force [46,47] as well as perturb the van der Waals attraction [47]. Using the Vold approach [48], the van der Waals energy of the spherical particles of a given radius (r), bearing a homogeneous surface layer of thickness (L) is given below:

$$V_{VDW} = -\frac{r}{12}\left[\frac{\left(\sqrt{A_s}-\sqrt{A_w}\right)^2}{H} + \frac{\left(\sqrt{A_p}-\sqrt{A_s}\right)^2}{H+2L} + 2\frac{\left(\sqrt{A_s}-\sqrt{A_w}\right)\left(\sqrt{A_p}-\sqrt{A_s}\right)}{H+L}\right] \tag{6}$$

where A_w, A_s and A_p refer to the Hamaker constants of the water, the surface layer, and the particle, respectively. Regarding the L value, the average adsorbed hydrodynamic layer thicknesses of the organic matter measured at the iron oxide surfaces was 1–2 nm [23,49]; this layer thickness depends on the solution pH. According to Au et al. [49], the value of 2 nm of layer thicknesses for pH 4.5 and 1 nm for pH 7.0 and 9.0 were used. As the Fe-M shows a similar adsorption behavior than the iron oxides [33], the same values were adopted here. Concerning the Hamaker constant of HA, the value

estimated by Bergstrom et al. [50] for hydrophilic cellulose was employed ($3.7\,E^{-20}$ J). Considering that the cellulose is a long-chain polymer, similar to HA, the value of Hamaker constant of cellulose could well represent the value for HA. The same approach was used by Séquaris [32].

It should be noted that the DLVO model has some limitations. Much evidence indicates that even in a simple system, classical DLVO theory is limited when attempting to describe the particle aggregation quantitatively; a sizable discrepancy still exists between theoretical predictions and experimental observations [8]. Even when other forces (i.e.: hydration, structural, hydrophobic, Born forces) are included in the model, the DLVO model does not fully match the experimental data. Some other possibilities of discrepancies are the dynamics of the interactions, surface roughness, discreteness of surface charge or the surface potential, and association in secondary minima [51]. This is why DLVO theory is seldom applied to clay mineral [30–32,52]. However, the DLVO model is widely used and applied to explain and predict the aggregation and deposition behavior of colloids and nanoparticles in aquatic environments [5–8,15,21,22,24,53]. In this work the DLVO model is only used as a theoretical framework to interpret the changes in the energy curves of Fe-M, related to the aggregation process under different experimental conditions, and not to assess quantitatively the aggregation of the Fe-M particles. That's beyond the scope of this work.

3. Results and discussion

3.1. Aggregation kinetics of colloidal aggregates of Fe-M: effect of particle concentration, pH, and ionic strength

The aggregation kinetics behavior of Fe-M depends on the effect of particle concentration, pH, and ionic strength. The effect of particle concentration was studied in order to evaluate the optimal particle concentration to use in aggregation experiments at different conditions (see supplementary material, SMl). The results obtained demonstrate that an increase in the particle concentration leads to a faster growth of aggregates, as indicated by an increase in R_h with time. To obtain the initial rate of aggregation, a linear least squares regression analysis was conducted, as was mentioned in Section 2.2. A significant change in the hydrodynamic radius with time was obtained for the highest concentration (20 mg L^{-1}), so this concentration was selected for all of the experiments (see SM1).

Fig. 1 a shows the pH-dependent aggregation rate of Fe-M at 0.01 M $NaNO_3$. At pH higher than 7, the initial rate of aggregation seems to be very similar, as the change in the hydrodynamic radius is almost the same (see SM2). As pH decreases, an increase in the hydrodynamic radius (and aggregation rate) is observed and aggregation of Fe-M is favored. This enhancement is important until pH 3. For pH < 3, the initial aggregation rate increases slowly (Fig. 1a), and the aggregation kinetic curve shows little change between pH 3 and 2.5 (see SM2). At very low pH (i.e: pH 2.5–3.0), the montmorillonite particles may dissolve [54], so that pH 4.0 was selected to obtain the rate of coagulation of Fe-M in the regime of fast aggregation (see next section). The aggregation behavior can be explained by the different nature of the surface charges that Fe-M was able to develop. As Fig. 1b shows, at all points of the studied pH range, the Fe-M has a dominant negative structural charge, present on the basal faces of Fe-M platelets. Only at pH lower than 5.0, a small decrease in zeta potential is observed, but the net charge remains negative. This slight decrease in zeta potential is a consequence of the pH-dependent surface charge on the edges. Although the development of a positive charge on the surface of the edges produced a little change in the negative net charge of Fe-M, this change was enough to generate some aggregation. Positively charged edges and

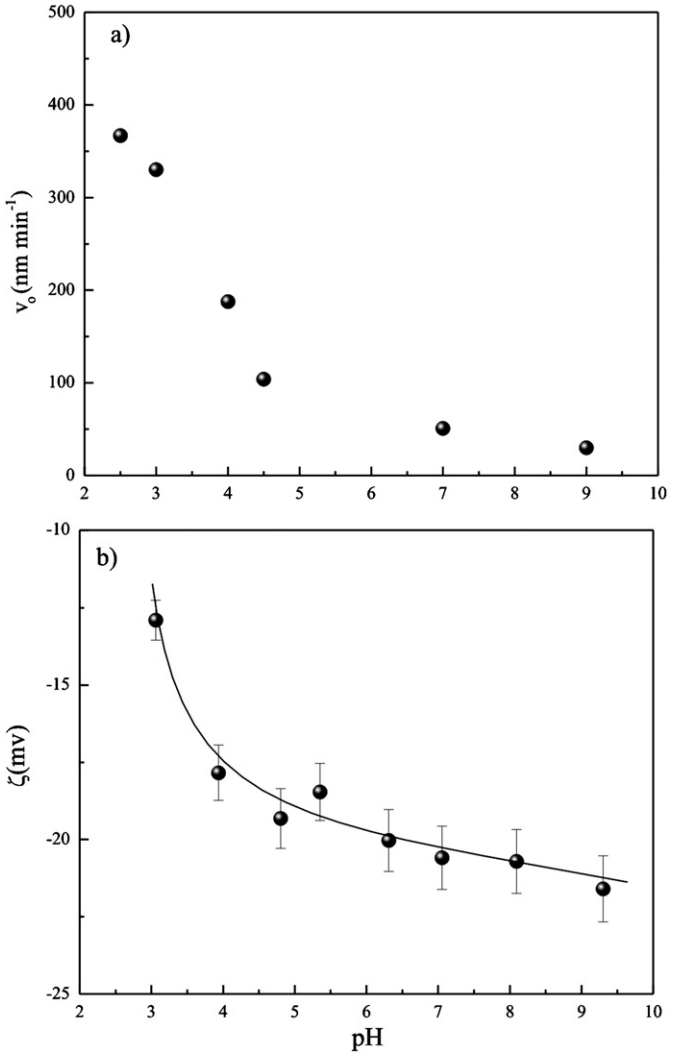

Fig. 1. (a) Initial aggregation rate as a function of pH, for Fe-M samples dispersed at 0.01 M $NaNO_3$. Solid concentration: 20 mg L^{-1}. (b) The zeta potential as a function of pH, for Fe-M samples dispersed at 0.01 M $NaNO_3$.

negatively charged faces of Fe-M could attract each other, resulting in the edge-to-face aggregation by electrostatic and van der Waals attractive interaction. When the suspension pH is increased above pH 6, the Fe-M surfaces are predominantly negatively charged and therefore edge-to-face aggregation by electrostatic attraction is no longer favorable; thus Fe-M particles are electrostatically stabilized. Under this situation, it would be expected that a concentration of electrolyte greater than 0.01 M is required to produce a face to face aggregation.

To investigate the effect of ionic strength in aggregation, the same experiment was conducted at a higher electrolyte concentration (0.02 and 0.04 M $NaNO_3$). The aggregation kinetic curves clearly show that the initial aggregation rate (and the change in the R_h) increase with electrolyte concentration (see SM3). The increase in aggregation with electrolyte concentration also depended on pH and, as seen with 0.01 M $NaNO_3$, this dependence is similarly correlated with surface charge (see SM4).

3.2. Stability ratio and critical coagulation concentration

The stability ratio for each experiment at different ionic strengths is shown in Fig. 2. The solid line represents fast aggregation ($W = 1$) and was determined for Fe-M suspended in 0.05 M

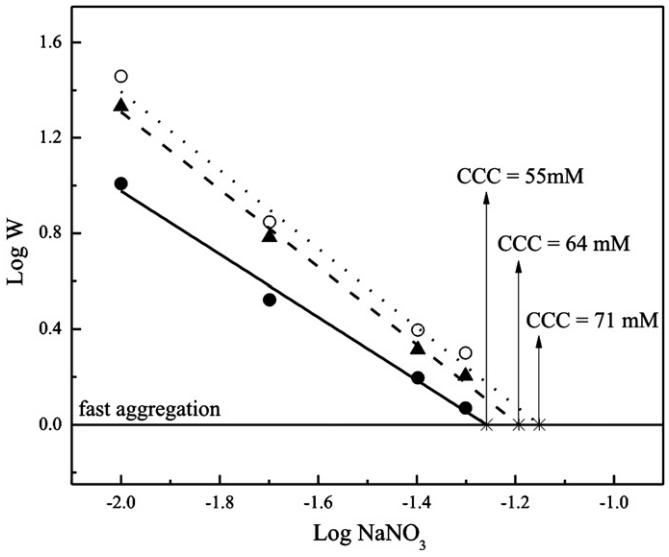

Fig. 2. Dependence of ionic strength on stability ratio (W) at pH 4.5 (solid circles), 7.0 (solid triangles) and 9.0 (open circle). The fast aggregation rate ($W = 1$) was determined experimentally as the aggregation rate of Fe-M suspended in 0.05 M $NaNO_3$ at pH 4.0.

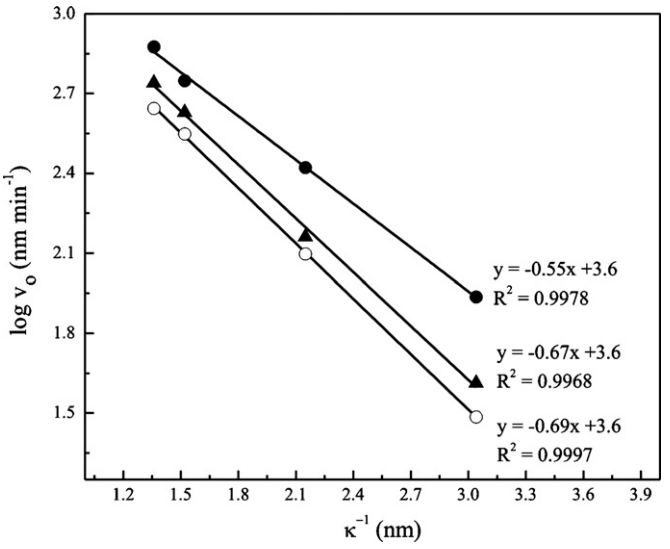

Fig. 3. Initial aggregation rate vs. the thickness of the double layer. Solid circles: pH 4.5, solid triangles: pH 7.0 and open circles: pH 9.0.

$NaNO_3$ at pH 4. At such a high electrolyte concentration the surface charge is well-screened, so every particle collision results in an attachment and $W = 1$. At lower electrolyte concentrations, where fast aggregation is not produced, the colloidal stability increases. As mentioned previously, the higher stability was obtained at pH 9.0 in 0.01 M $NaNO_3$. Thus, to produce a well-dispersed suspension of Fe-M, the optimal required conditions are a low ionic strength and a high pH value.

The critical coagulation concentration (CCC) can be determined from the graphic of $\log_{10} W$ as a function of $\log_{10}$ofelectrolyte concentration [55]. This graph consists in two intersecting straight lines, which represents two distinct regimes: reaction and diffusion limited regimes. The CCC can be obtained by determining the intersection point between these regimes. It is noteworthy here that other experiments were carried out at higher ionic strength (e.g.: 60 mM). However, there was a large scatter in the data obtained (the upper limit of the equipment used for determining the particle size is 6000 nm-diameter). For the experiments performed, these two regions could not to be distinguished (Fig. 2) ; therefore the CCC value was obtained by extrapolating the value of the electrolyte concentration for which $W = 1$ (Fig. 2). According to the experimental results, the CCC values obtained for Fe-M at each pH studied are 55, 64, and 71 mM for pH 4.5, 7.0, and 9.0 respectively. The CCC values obtained in this study are of the same order of magnitude as the values obtained for other similar montmorillonites, informed by other authors. Tombáck and Szekeres [56] obtained values of 25, 52 and 97 mM for a Na-M in NaCl at pH 4, 6 and 8.5 respectively. Golberg et al. [57] found a slightly lower value (32 mM) for a Na-M at pH 9, similar than the value obtained by Lagaly and Ziesmer [58] (20 mM) at pH 6.5. By using a kinetic aggregation method, Garcia et al. [30] obtained a value of 0.7 M at pH 8, which is higher than the value obtained in this study.

As mentioned above, the effect of ionic strengths on aggregation is related with a well-screened surface charge that promotes aggregation. At low pH values, attractive electrostatic forces predominate and edge-to-face aggregation is produced. As pH increases, edge surface is negatively charged and edge-to-face aggregation is limited, and the dispersion is electrostatically stabilized. When the electrolyte concentration is increased, the negative surface charge of Fe-M could be well-screened; the thickness of the double layer is reduced and the face-to-face or edge-to-face aggregation is promoted. This effect is displayed in Fig. 3. Here, the log values of the initial aggregation rate ($\log \nu_0$) appear to be linearly dependent on the thickness of the double layer (κ^{-1}). The relation between them seems to be very similar for pH levels of 7.0 and 9.0, while for pH 4.5 is less intense. These differences are related to the conditions that the system has for each pH; low pH is not entirely dispersed (in 0.01 M $NaNO_3$), while the system at pH 7.0 and 9.0 was well dispersed.

3.3. *Effect of pH and ionic strength on the stability of Fe-M: analysis with the DLVO theory*

The DLVO theory was employed to explain the changes in the total potential energy of Fe-M particles, and their interaction under different conditions. Short-range forces, such as the Born and hydration forces, are not taken into account, as they are significant only at distances shorter than the position of the maxima displayed by the balance between the electrostatic and the van der Waals energies [55]. As was mentioned, the spherical geometry was used to approximate the shape of the Fe-M particles. Prior to making this approach, the corresponding equations describing the van der Waals interaction between two plane surfaces was attempted [55]. However, the DLVO energy profiles obtained do not depict the experimental results (i.e.: the net interaction energy obtained was always attractive, whatever the pH evaluated). García et al. [30] also mentioned that if using planar geometry, the DLVO theory fails to describe previous experimental observations on the montmorillonite system, which can be excellently reproduced using spherical geometry. Therefore, the approximation of a spherical geometry has also been adopted here.

In order to simulate the general trend of the experimental aggregation data, the theoretical stability ratio (or the attachment efficiency, α) could be calculated using the DLVO theory and then be compared with the experimentally obtained value. Some authors use this approach [6,59]. When the system is relatively monodispersed, DLVO theory can explain the experimental values [6,59]. However, in many other cases, predictions are different from the measured values [60]. Hahn and O'Melia [60] used a Maxwell approach to estimate the particle collision efficiency. They pointed out that predictions of the attachment efficiency are many orders of magnitude smaller than measured values, and that the inclusion of hydration, structural, hydrophobic, Born, or other forces in

modeling does not fully correct the predictions. The authors mentioned that other possibilities, such us the dynamics of the interactions, surface roughness, discreteness of surface charge or surface potential, and association in secondary minima may be responsible of the discrepancy between theoretical and experimental values. This seems to be the situation for the Fe-M particles, where the attachment efficiency predictions are smaller than the experimental values. Therefore, as noted above, DLVO profiles obtained in this study were used only for the purpose of qualitatively explaining and describing the aggregation of particles of Fe-M. Bearing in mind this, the DLVO energy profiles for Fe-M–Fe-M particle interactions as a function of solution pH and ionic strength are shown in Fig. 4. As a general feature, the total interaction energy profiles presents a deep attractive primary energy minimum (Φ_{1min}) of theoretically infinite depth at short separation distances (not shown here), a primary repulsive energy maximum (Φ_{max}) at a larger separation distance and a comparatively smaller attractive secondary energy minimum (Φ_{2min}) at an even larger separation distance. The energy barrier, which is used to estimate stability, refers to the difference between Φ_{max} and Φ_{2min} [16,60,61]. Particles that overcome the energy barrier will aggregate irreversibly with other particles in the deep primary energy minimum, at a short separation distance (<3 nm). The secondary minimum, in which weak aggregation is possible, can occur at a larger separation distance. DLVO profiles shown in Fig. 4 clearly illustrate that the attractive interaction increases markedly with ionic strength and low pH values; the particles become attracted to each other, so the colloid turns unstable. In addition, for pH 4.5 at 0.04 M $NaNO_3$,an effective low Φ_{max} height (1.7 kT) for coagulation can be obtained. Under solution conditions where Φ_{max} is lower than the average thermal energy of particles (1.5 kT), an effective coagulation of the Fe-M particles can be expected [61]. However, the hallmark of all Fe-M-DLVO profiles is the presence of the secondary minimum. It could be also observed in Fig. 4 how the magnitude of the secondary minimum is enhanced, when the ionic strength and pH increases. The energy barriers observed for all the conditions are very high (above 10 kT) preventing aggregation into the primary energy minimum [61]. Therefore, the secondary energy minimum should control colloid aggregation in this system.

Hahn et al. [62][62 and references therein] explained how the aggregation can occur in the primary or secondary minimum, depending on the particle size of the colloid particle. For particles less that a few tens of nanometers in diameter, the aggregation occurs in primary minimum. For particles larger, stability decreases with increasing particle size and the aggregation occurs in the secondary minimum. The R_h of Fe-M in the stable condition is large enough to justify that the association in the secondary minimum may occur. In general, colloids that associate in the secondary minimum are considered reversibly attached, when the secondary energy minimum (Φ_{2min}) is comparable to the average Brownian kinetic energy [62]. This means that, if the energy barrier height is higher than 10 kT and the particles have enough kinetic energy, they could be aggregated in the secondary minimum and then be disaggregated again. Under these conditions the process is readily reversed. For the Fe-M particles, the value of the secondary energy minimum is higher than the average particle Brownian kinetic energy, suggesting that the attraction within the secondary minimum was not reversed.

The relationship between Φ_{max}, Φ_{2min} and ionic strength is displayed in Fig. 5. In any of the pH and ionic strength ranges studied, not a linear relationship is observed. The energy barrier decreases slowly as the ionic strength increase, but starting at 0.04 M the interaction energy falls fast until reaching the zero Φ_{max} energy. This energy value is corresponds to the CCC value, where the fast aggregation process occurs and the interactions between colloids are attractive at any separation distance. Fig.5 shows that the Φ_{max}

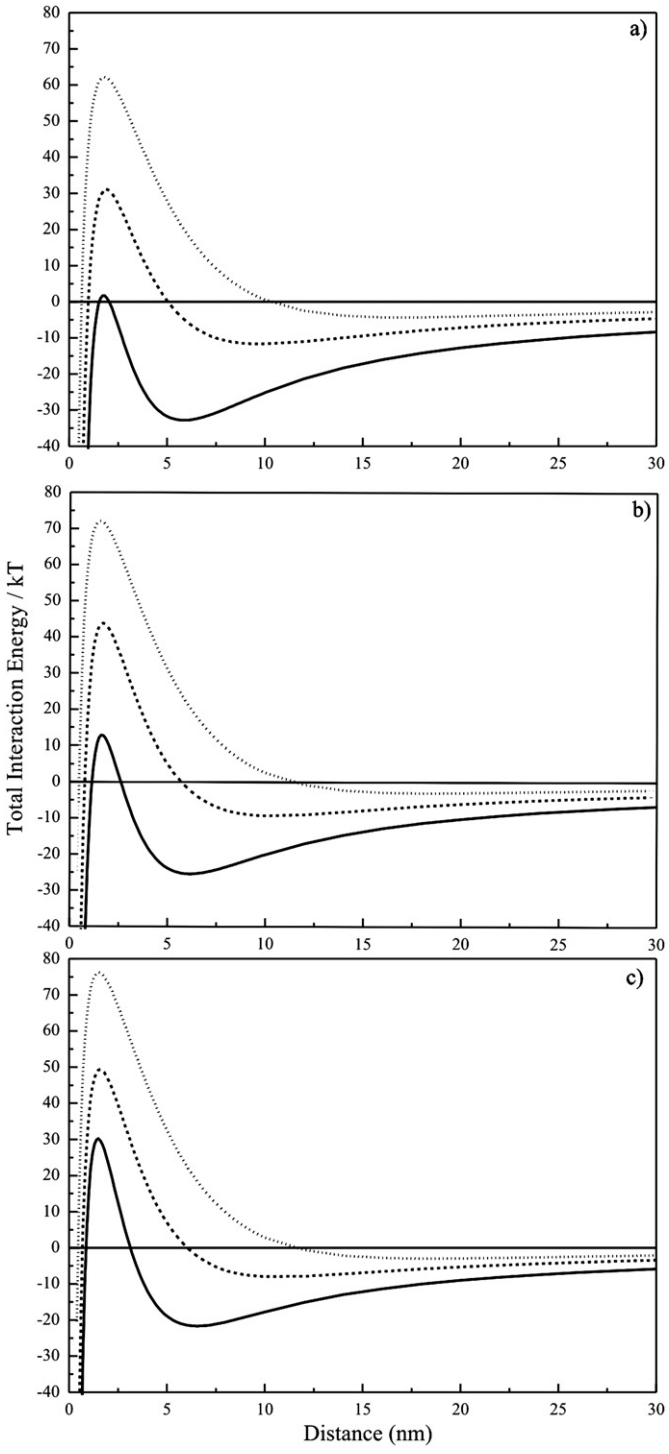

Fig. 4. DLVO interaction energy profiles for suspensions of Fe-M at pH 4.5 (a), 7.0 (b) and 9.0 (c). Solid line: 0.04 M $NaNO_3$; dash line: 0.02 M $NaNO_3$; dot line: 0.01 M $NaNO_3$.

energy of Fe-M at pH 4.5 and 0.04 M is very low and close to CCC conditions, and the transition from the slow to fast aggregation requires an increase of ionic strength. A similar behavior is displayed in the Fe-M particles at pH 7.0 and 9.0, but in these cases the decrease in the interaction energy seems to be less pronounced due to the improved stability conditions of the system at higher pH values.

Considering all the above, the following assumptions can be made: under at all conditions evaluated, the energy barrier is not

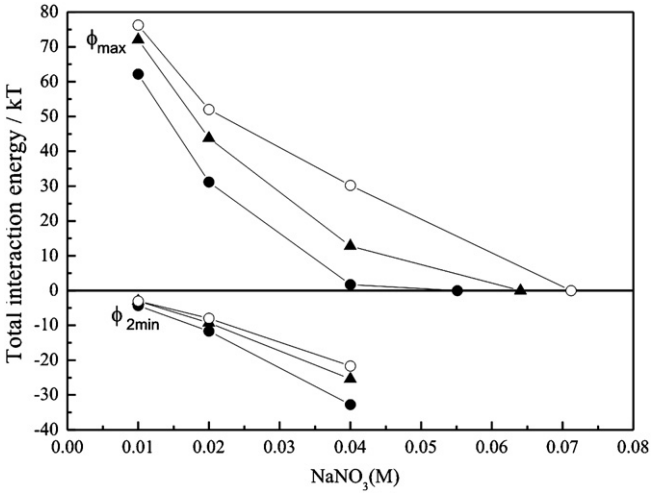

Fig. 5. Dependence of energy barrier with ionic strength for pH 4.5 (solid circles) ; pH 7.0 (solid triangles) and pH 9.0 (open circles).

high enough to produce aggregation in the primary minimum. Hence, the secondary energy minimum controls the aggregation process for the Fe-M particles. Besides, the secondary energy minimum value suggests that this process is not reversed. In view of the above, it is possible to assume that the aggregation rate of the initial Fe-M particles is always high enough to produce several small aggregate nuclei, irreversibly on the secondary minimum. However, the particles have enough potential energy to maintain stable the suspension and not coagulate. Then, when pH or ionic strength is strongly modified, these small nuclei aggregates may aggregate further, resulting in the coagulation of the suspension.

It is worth noting that the application of the DLVO model to the prediction of the clay colloidal stability at pH 4.5 implies some uncertainty [63]. At pH < 6.5, the layers and the edges are opposite signs and aggregation effects between edges and faces are responsible for lower stability. Since the absolute value of the charge developed at the edges of the particle is much smaller than the permanent negative value, it can only induce a very small variation in the magnitude of the zeta potential. The magnitude of the pH-dependent charge is very small compared to that of the permanent charge, so in the DLVO model its effects can be observed, but only slightly.

3.4. Effect of HA on the colloidal stability of Fe-M: experimental and DLVO prediction

The effect of HA on Fe-M aggregation as a function of solution pH and ionic strength was evaluated. Data for aggregation rates at pH 4.5, 7.0, and 9.0 and for 0.01 M $NaNO_3$ are present in SM5. Small amounts of HA in the Fe-M suspension result in a decrease of aggregation rates. This effect is more intense at pH 4.5 (see SM5), where the suspension is less stable. For all pH values, the addition of 2 mg L^{-1} produces a decrease in the aggregation rates, while amounts of 10–20 mg L^{-1} almost doesn't change the colloidal stability, since the R_h (and the aggregation rate value) obtained at pH 4.5 are close to the values obtained at pH 9.0, in absence of HA (see Fig. 1). This effect is more pronounced at higher ionic strengths (not shown here). For pH 7.0 and 9.0, the effect of HA on aggregation was less important.

It is well known that humic substances are negatively charged polyelectrolyte with predominantly carboxylic and phenolic type functional groups. Because they are negatively charged at all pH, its adsorption onto oxides and clays is depended on pH, increasing as pH decrease [64]. HA adsorption affects particle stability in two principal ways. First, it modifies the effective interfacial charge and thus the magnitude and possibly signs of the electrostatic interactions between the surfaces. Second, steric barriers (due to the large size of HA molecule) which prevent interparticle approaches and diminish the impact of attractive van der Waals interactions [22]. Steric repulsion is dominant at very small separation distances (<10 nm), at high ionic strength, as well as at pH values near the pH_{PZC} when electrostatic repulsion is absent or minimal [65].

The degree to which HA adsorption alters particle stability is dependent on the solution chemistry and the characteristics of the particle and the HA molecule. Under acidic conditions, the adsorption of HA to the edges of Fe-M particles can cause changes in the net surface charge; the protonated surface of the edges reverses its positive charge to negative. This effect can barely be observed in the zeta potential data in presence of different HA concentrations at pH 7.0 and 9.0, but is more evident at pH 4.5 (see SM5). As a result of this adsorption, edge-to-face aggregation is prevented. The electrical charges of attached HA screen the attraction; thus the colloidal stability is increased due to the electrostatic stabilization produced by the reversal of the edge positive charge.

The steric stabilization of colloids due to the adsorption of HA molecule have been also investigated and modeled [24,26,32]. To evaluate the significance of the steric stabilization for the Fe-M system, a simple model was applied [48]. The model takes into account the effect of the bearing surface layer thickness of the HA attached to the Fe-M particles.

Fig. 6 shows the DLVO energy profiles for the Fe-M-HA particles' interactions as a function of solution pH and ionic strength in the presence of HA. For comparative purposes, only the data for 2 and 20 mg L^{-1} of HA added and 0.01 and 0.04 M $NaNO_3$ has been plotted. In all studied cases, the stabilization occurs and the system becomes more stable with higher values of energy barrier, in contrast to those results obtained in absence of HA (Fig. 4). The increase in stability is more important for pH 4.5 at 0.04 M $NaNO_3$, where the suspension stability is very low and very near to the condition of fast aggregation. For pH 7.0 and 9.0, the addition of HA did not increase the Fe-M stability as much, since the energy barriers were large enough to maintain the stability of the suspension. In terms of energy interactions, the increased electrostatic repulsion between particles, due to the adsorption of HA, results in higher repulsive energy barriers and in shallower attractive secondary minima.

Comparing the steric stabilization due to adsorbed HA with the electrostatic effect in stabilizing the Fe-M suspension, HA absorbed has an important influence at any pH studied, although it is more important at pH 4.5 and higher ionic strength (i.e.: at pH 4.5 and ionic strength of 0.04 M the steric stabilization is more important than the effect of reducing only the ionic strength from 0.04 to 0.01 M). Less influence has at 0.01 M; under such conditions the system is already stable and the addition of HA does not increase so much the stability of the system. However, for the three pH levels studied, the suspension of the Fe-M reached similar values of the total interaction energy due to the combination of both factors, so the same stability could be achieved suggesting that the Fe-M reached the most stable colloidal conditions.

It is worth mentioning here that, beyond 5 nm distances between the Fe-M particles the second minimum is also present. As was mentioned above, this secondary minima is shallower as the HA diminish the attractive interaction. However the secondary energy minimum value is still high enough to produce an irreversible aggregation in the secondary minima.

Fig. 7 shows the increase in CCC values as the amount of HA increases. As previously noted, for the higher amounts of HA added to the system, the CCC values obtained for the three pH studied are very similar, indicating similar states of stability under these conditions.

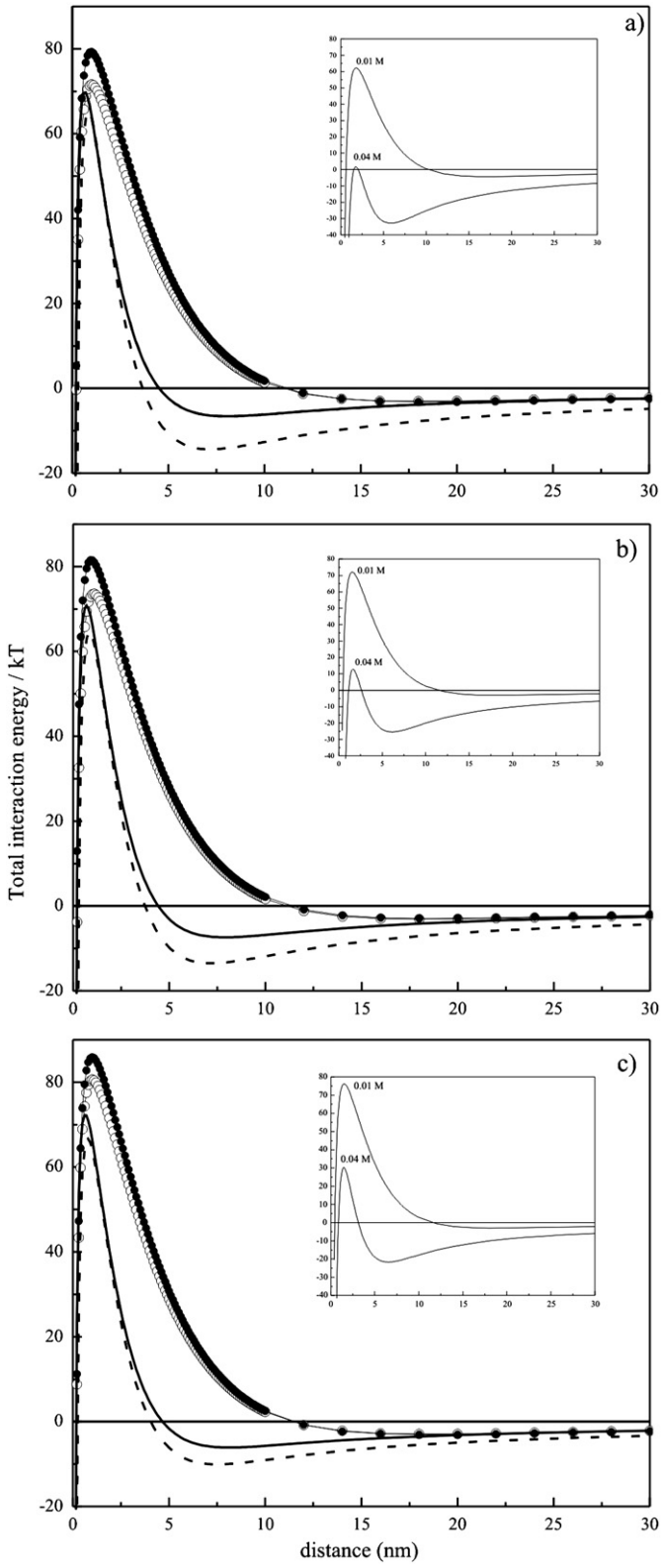

Fig. 6. DLVO interaction energy profiles for suspensions of Fe-M in the presence of HA as a function of pH: 4.5 (a), 7.0 (b), 9.0 (c) and ionic strength. Solid circles: 20 mg L^{-1} of HA in 0.01 M $NaNO_3$. Open circles: 2 mg L^{-1} of HA in 0.01 M $NaNO_3$. Solid line: 20 mg L^{-1} of HA in 0.04 M $NaNO_3$. Dash line: 2 mg L^{-1} of HA in 0.04 M $NaNO_3$. Inset in figures: comparison of DLVO interaction energy profiles in absence of HA, for two ionic strengths.

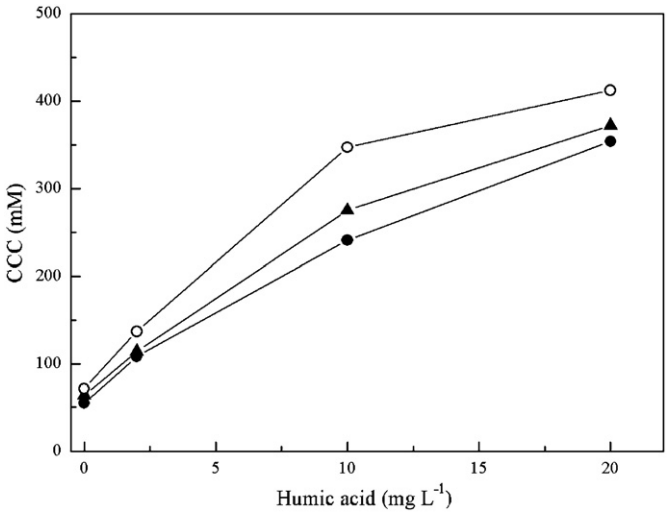

Fig. 7. Effect of HA on CCC of Fe-M at pH 4.5 (solid circles), 7.0 (solid triangles) and 9.0 (open circles).

4. Conclusions and environmental implications of particles aggregation

The aggregation kinetics of Fe-M particles under different levels of organic matter, ionic strengths and pH conditions were investigated through experimental techniques and DLVO calculations. This study demonstrates that low pH and high ionic strength may destabilize Fe-M suspensions by altering the surface charge, which results in a minor energy barrier which must be overcome and a deeper secondary minimum energy. HA has an opposite effect, stabilizing the Fe-M suspension at any pH. The stability of the suspension for the three pH levels studied increases as HA increases until reaching a maximum of level of stabilization, where the concentration needed to produce aggregation is almost the same. The concentration effect of HA has further been proved via the observing the change of the energy barrier in DLVO profiles, when the concentration of HA is increased. When comparing the steric and electrostatic effects on the Fe-M stabilization, both have an important influence for all pH levels studied, although steric is more pronounced at pH 4.5 and high ionic strength.

To a large extent, the transport of common environmental pollutants occurs through water, either directly as dissolved compounds, or by using suspended materials as vectors. Soils, sediments and water bodies contain solid and dissolved matter which can be powerful geo-adsorbents. Environmental factors such as pH and ionic strengths, together with the physical–chemical properties, structure and concentration of such geo-adsorbents may determine whether pollutans are bound within or transported out of soils and sediments. Fe-M is a natural colloid which is commonly present in natural waters. All of these factors influence its adsorption capacity, but its ability to transport pollutants over distances can also depend on its stability. The results obtained show that at pH 7.0 and 9.0 (pH range of natural water) the Fe-M particles are stabilized. Under more acidic conditions, edge-to-face aggregation could be occurring, causing two main effects: (1) particles may set down and therefore stop their transport over distances; (2) surface groups that could adsorb contaminants are blocked. Experimental data and predictions also show that the presence of an HA layer with an average thickness of about 1–2 nm can produce a steric stabilization of dispersed Fe-M particles. This means that not only surface-coating stabilized clay minerals but also blocked surface sites available for adsorption. On the other hand, an increasing salt concentration may ignite the Fe-M aggregation. This process typically occurs when

river water reaches the high salt concentrations of the sea. For our system, a concentration of 55 mM, 64 and 71 mM for pH 4.5, 7.0 and 9.0 are necessary to produce coagulation of Fe-M particles. These values are commonly found in naturally saline médiums.

Acknowledgments

This work was financed by Argentina's FONCYT, SECYT-UNC and CONICET. L. Borgnino is member of CICyT in Argentina's CONICET. Language assistance by native English speaker Wendy Walker is gratefully acknowledged. I am especially grateful to the anonymous reviewers for suggesting significant improvements to this manuscript.

Appendix A. Supplementary data

Supplementary data associated with this article can be found, in the online version, at http://dx.doi.org/10.1016/j.colsurfa.2013.01.065.

References

[1] J.J. Stumm, W. Morgan, in: Aquatic Chemistry, Wiley-Interscience, New York, 1996.
[2] J.F. McCarthy, J.M. Zachara, Subsurface transport of contaminants, Environ. Sci. Technol. 23 (1989) 496–502.
[3] J. Ren, A.I. Packman, Modeling of simultaneous exchange of colloids and sorbing contaminants between streams and streambeds, Environ. Sci. Technol. 38 (2004), 2901-291.
[4] G. Benjamin, L. Guoping, S.K. Christopher, Stable cluster formation in aqueous suspensions of iron oxyhydroxides nanoparticles, J. Colloid Interface Sci. 313 (2007) 152–159.
[5] Y.T. He, J. Wan, T. Tokunaga, Kinetic stability of hematite nanoparticles: the effect of particle sizes, J. Nanopart. Res. 10 (2008) 321–332.
[6] X. Liu, M. Wazne, C. Christodoulatos, K.L. Jasinkiewicz, Aggregation and deposition behavior of boron nanoparticles in porous media, J. Colloid Interface Sci. 330 (2009) 90–96.
[7] A.A. Keller, H. Wang, D. Zhou, H.S. Lenigan, G. Cherr, B.J. Cardinbale, R. Miller, J. Zhaoxia, Stability and aggregation of metal oxide nanoparticles in natural aqueous matrices, Environ. Sci. Technol. 44 (2010) 1962–1967.
[8] K. Li, Y. Chen, Effect of natural organic matter on the aggregation kinetics of CeO_2 nanoparticles in KCl and $CaCl_2$ solutions: measurements and modeling, J. Hazard. Mater. 209–210 (2012) 264–270.
[9] H. van Olphen, in: An Introduction to Clay Colloid Chemistry, Interscience Publishers, Div. of John Wiley & Sons, 605 Third Ave, New York 16, N. Y, 1963.
[10] M. Elimelech, C.R. O'Melia, Kinetics of deposition of colloidal particles in porous media, Environ. Sci. Technol. 24 (1990) 1528–1556.
[11] M. Elimelech, C.R. O'Melia, Effect of particle size on collision efficiency in the deposition of Brownian particles with electrostatic energy barriers, Langmuir 6 (1990) 1153–1163.
[12] M. Elimelech, J. Gregory, J.X. Jia, R.J. Williams, in: Particle deposition and aggregation: measurement, modelling and simulation, Oxford, Butterworth-Heinemann, 1995.
[13] A.P. Nicholas, D.E. Walling, The significance of particle aggregation in the overbank deposition of suspended sediment on river floodplains, J. Hydrol. 186 (1996) 275–293.
[14] E. Tombácz, G. Filipcsei, M. Szekeres, Z. Gingl, Particle aggregation in complex aquatic systems, Colloids Surf. A 151 (1999) 233–244.
[15] S.E. Mylon, K.L. Chen, M. Elimelech, Influence of natural organic matter and ionic composition on the kinetics and structure of hematite colloid aggregation: implications to iron depletion in estuaries, Langmuir 20 (2004) 9000–9006.
[16] A. Franchi, C.R. O'Melia, Effects of natural organic matter and solution chemistry on the deposition and reentrainment of colloids in porous media, Environ. Sci. Technol. 37 (2003) 1122–1129.
[17] B.V. Derjaguin, L. Landau, Theory of stability of strongly charged lyophobic sols and of the adhesion of strongly charged particles in solutions of electrolytes, Acta Physicochim. URSS 14 (1941) 633–662.
[18] E.J.W. Verwey, J.T.P. Overbeek, in: Theory of the Stability of Lyophobic Colloids. The Interaction of Particles having an Electric Double Layer, Elsevier, New York-Amsterdam, 1948.
[19] S.N. Liss, I.G. Droppo, D.T. Flannigan, G.G. Leppard, Floc architecture in wastewater and natural riverine systems, Environ. Sci. Technol. 30 (1996) 680–686.
[20] J.M. Fox, P.S. Hill, T.G. Milligan, A. Boldrin, Flocculation and sedimentation on the Po River Delta, Mar. Geol. 203 (2004) 95–107.
[21] K.L. Chen, S.E. Mylon, M. Elimelech, Aggregation kinetics of alginate-coated hematite nanoparticles in monovalent and divalent electrolytes, Environ. Sci. Technol. 40 (2006) 1516–1523.
[22] K.L. Chen, M. Elimelech, Influence of humic acid on the aggregation kinetics of fullerene (C60) nanoparticles in monovalent and divalent electrolyte solutions, J. Colloid Interface Sci. 309 (2007) 126–134.
[23] M. Baalousha, A. Manciulea, S. Cumberland, K. Kendall, J.R. Lead, Aggregation and surface properties of iron oxide nanoparticles; influence of pH and natural organic matter, Environ. Toxicol. Chem. 27 (2008) 1875–1882.
[24] M. Baalousha, Aggregation and disaggregation of iron oxide nanoparticles: influence of particle concentration, pH and natural organic matter, Sci. Total Environ. 40 (2009) 2093–2101.
[25] J.-D. Hu, Y. Zevi, X.-M. Kou, J. Xiao, X.-J. Wang, Y. Jin, Effect of dissolved organic matter on the stability of magnetite nanoparticles under different pH and ionic strength conditions, Sci. Total Environ. 408 (2010) 3477–3489.
[26] R. Kretzschmar, H. Holthoff, H. Sticher, Influence of pH and humic acid on coagulation kinetics of kaolinite: a dynamic light scattering study, J. Colloid Interface Sci. 202 (1998) 95–103.
[27] C.A. Aurell, A.O. Wistrom, Coagulation of kaolinite colloids in high carbonate strength water, Colloids Surf. A: Physicochem. Eng. Aspects 168 (2000) 277–285.
[28] G. Lagaly, S. Ziesmer, Colloid chemistry of clay minerals: the coagulation of montmorillonite dispersions, Adv. Colloid Interface Sci. 100–102 (2003) 105–128.
[29] L. Heidmann, I. Cristl, R. Kretzachmar, Aggregation kinetics of kaolinite–fulvic acid colloids as affected by the sorption of Cu and Pb, Environ. Sci. Technol. 39 (2005) 807–813.
[30] S. García-García, S. Wold, M. Jonsson, Kinetic determination of critical coagulation concentrations for sodium- and calcium-montmorillonite colloids in NaCl and $CaCl_2$ aqueous solutions, J. Colloid Interface Sci. 315 (2007) 512–519.
[31] Y. Furukawa, J.L. Watkins, J. Kim, K.L. Curry, R.H. Bennett, Aggregation of montmorillonite and organic matter in aqueous media containing artificial seawater, Geochem. Trans. 10 (2009) 1–11.
[32] J.-M. Séquaris, Modeling the effects of Ca^{2+} and clay-associated organic carbon on the stability of colloids from topsoils, J. Colloid Sci. 343 (2010) 408–414.
[33] L. Borgnino, M. Avena, C.P. De Pauli, Synthesis and characterization of Fe(III)-montmorillonites for phosphate adsorption, Colloids Surf. A 341 (2009) 46–52.
[34] L. Borgnino, C.E. Giacomelli, M.J. Avena, C.P. De Pauli, Phosphate adsorbed on Fe(III) modified montmorillonite: surface complexation by ATR-FTIR spectroscopy, Colloids Surf. A 353 (2010) 238–244.
[35] G. Bia, C.P. De Pauli, L. Borgnino, The role of Fe(III) modified montmorillonite on fluoride mobility: adsorption experiments and competition with phosphate, J. Environ. Manage. 100 (2012) 1–9.
[36] M.J. Avena, L. Valenti, V. Pfaffen, C.P. De Pauli, Methylene blue dimerization does not interference in surface-area measurements of kaolinite and soils, Clays Clay Miner. 49 (2001) 168–173.
[37] D.L. Sparks, J.M. Bartels, J.M. Bigham (Eds.), Methods of Soil Analysis, Soil Science Society of America, Madison WI, USA, 1996, p. 1018.
[38] H. Holthoff, S.U. Egelhaaf, M. Borkovec, P. Schurtenberger, H. Sticher, Influence of pH and humic acid on coagulation kinetics of kaolinite: a dynamic light scattering study, Langmuir 12 (1996) 5541–5549.
[39] K.A. Huynh, K.L. Chen, Aggregation kinetics of citrate and polyvinylpyrrolidone coated silver nanoparticles in monovalent and divalent electrolyte solutions, Environ. Sci. Technol. 45 (2011) 5564–5571.
[40] J. Gregory, in: Particles in Water: Properties and Processes, IWA Publishing, CRC Press, London, Boca Raton, 2006.
[41] R. Hogg, T.W. Healy, D.W. Fuerstenau, Mutual coagulation of colloidal dispersions, Trans. Faraday Soc. 62 (1966) 1638–1651.
[42] M. Elimelech, J. Gregory, G. Jia, R. Williams, in: Surface Interaction Potentials, Butterworth–Heinemann, Woburn, MA, USA, 1995.
[43] K. Norrish, The swelling of montmorillonite, Discuss. Faraday Soc. 18 (1954) 120–134.
[44] J.D.G. Durán, M.M. Ramos-Tejada, F.J. Arroyo, F. González-Caballero, Rheological and electrokinetic properties of sodium montmorillonite suspensions Part I: rheological properties and interparticle energy of interaction, J. Colloid Interface Sci. 229 (2000) 107–117.
[45] D. Grasso, K. Subramaniam, M. Butkus, K. Strevett, J. Bergendahl, A review of non-DLVO interactions in environmental colloidal systems, Rev. Environ. Sci. Biotechnol. 1 (2002) 17–38.
[46] T.L. Byrd, J.Y. Walz, Interaction force profiles between *Cryptosporidium parvum* oocysts and silica surfaces, Environ. Sci. Technol. 39 (2005) 9574–9582.
[47] V. Runkana, P. Somasundaran, P.C. Kapur, A population balance model for flocculation of colloidal suspensions by polymer bridging, Chem. Eng. Sci. 61 (2006) 182–191.
[48] M.J. Vold, The effect of adsorption on the van der waals interaction of spherical colloidal particles, J. Colloid Sci. 16 (1961) 1–12.
[49] K.-K. Au, A.C. Penisson, S. Yang, C.R. O'Melia, Natural organic matter at oxide–water interfaces, Geochim. Cosmochim. Acta 63 (1999) 2903–2917.
[50] L. Bergström, S. Stemme, T. Dahlfors, H. Arwin, L. Ödberg, Spectroscopy ellipsometry characterization and estimation of the Hamaker constant of cellulose, Cellulose 6 (1999) 1–10.
[51] M.W. Hahn, C.R. O'Melia, Deposition and reentrainment of Brownian particles in porous media under unfavorable chemical conditions: some concepts and applications, Environ. Sci. Technol. 38 (2004) 210–220.
[52] A. Nosrati, J. Addai- Mensah, W. Skinner, Muscovite clay mineral particle interactions in aqueous media, Powder Technol. 219 (2012) 228–238.

[53] A.R. Petosa, D. Jaisi, I.R. Quevedo, M. Elimelech, N. Tufenkji, Aggregation and deposition of engineered nanomaterials in aquatic environments: role of physicochemical interactions, Environ. Sci. Technol. 44 (2010) 6532–6549.
[54] M.L. Rozalén, F.J. Huertas, P.V. Brady, J. Cama, S. García-Palma, J. Linares, Experimental study of the effect of pH on the kinetics of montmorillonite dissolution at 25 °C, Geochim. Cosmochim. Acta 72 (2008) 4224–4234.
[55] R.J. Hunter, Foundations of Colloid Science, vol I, Oxford University Press, New York, 1993.
[56] E. Tombácz, M. Szekeres, Colloidal behavior of aqueous montmorillonite suspensions: the specific role of pH in the presence of indifferent electrolytes, Appl. Clay Sci. 27 (2004) 75–94.
[57] S. Golberg, H.S. Forster, E. Heick, Flocculation of illite/kaolinite and illite/montmorillonite mixtures as affected by sodium adsorption ratio and pH, Clays Clay Miner. 39 (1991) 375–380.
[58] G. Lagaly, S. Ziesmer, Colloid chemistry of clay minerals: the coagulation of montmorillonite dispersions, Adv. Colloid Interface Sci. 100-102 (2003) 105–115, OLDBERG, HAROLD S. FORSTER, AND E.
[59] K.A. Huynh, K.L. Chen, Aggregation kinetics of citrate and polyvinylpyrrolidone coated silver nanoparticles in monovalent and divalent electrolyte solutions, Environ. Sci. Technol. 45 (2011) 5564–5571.
[60] M.W. Hahn, C.R. O'Melia, Deposition and reentrainment of Brownian particles in porous media under unfavorable chemical conditions: some concepts and applications, Environ. Sci. Technol. 38 (2004) 210–220.
[61] J.N. Israelachvili, in: Intermolecular and Surface Forces, Academic Press, London, 1992.
[62] M.W. Hahn, D. Abadzic, C.R. O'Melia, on the role of secondary minima, Environ. Sci. Technol. 38 (2004) 5915–5924.
[63] T. Missana, A.J. Adell, On the applicability of DLVO theory to the prediction of clay colloids stability, Colloid Interface Sci. 230 (2000) 150–156.
[64] L. Weng, W.H. Van Riemsdijk, T. Hiemstra, Adsorption of humic acids onto goethite: effects of molar mass, pH and ionic strength, J. Colloid Interface Sci. 314 (2007) 107–118.
[65] L.M. Mosley, K.A. Hunter, W.A. Ducker, Forces between colloid particles in natural waters, Environ. Sci. Technol. 37 (2003) 3303–3308.